

## Si diffusion in GaAs and Si-induced interdiffusion in GaAs/AlAs superlattices

B. Chen, Q.-M. Zhang, and J. Bernholc

*Department of Physics, North Carolina State University, Raleigh, North Carolina 27695-8202*

(Received 9 September 1993)

Various microscopic mechanisms for Si diffusion in GaAs and Si-induced interdiffusion in GaAs/AlAs superlattices are investigated by *ab initio* molecular dynamics. The dominant mechanism involves the motion of negatively charged  $\text{Si}_{\text{III}}-\text{V}_{\text{III}}$  pairs through second-nearest-neighbor jumps. This mechanism explains both the ability of Si to disorder superlattices regardless of whether it was introduced during growth or in-diffused afterwards and the suppression of interdiffusion by compensation doping. The computed activation energies are in very good agreement with the experimental data.

Understanding of the interplay between the motion of impurities, doping, and material composition in compound semiconductors is both of fundamental interest and substantial utility in designing device structures and materials. As a main *n*-type dopant, Si in GaAs has been extensively investigated. Various mechanisms of its diffusion have been proposed and both experimental and theoretical investigations exist.<sup>1</sup> Nevertheless, the dominant pathway(s) governing its motion have not yet been determined. Si diffusion can also lead to a disordering of GaAs/AlAs superlattices<sup>2,3</sup> well below the intrinsic interdiffusion temperature, and thus have applications in the patterning of device structures. The various impurity-induced disordering (IID) phenomena have been intensively studied and a wealth of data exists, most of which still awaits a mechanistic explanation. Although both *p*- and *n*-type impurities can cause IID, the underlying mechanisms can be completely different. For acceptors at moderate concentrations, IID occurs only when they are in-diffused from the surface; whereas for donors in significant concentrations it occurs regardless of whether they were introduced during the growth or in-diffused afterwards.<sup>1</sup> In this paper, Si diffusion in GaAs and Si-related IID is investigated by large-scale *ab initio* calculations. The results provide a mechanistic understanding of Si diffusion and of Si-induced interdiffusion. They may also be applicable to IID involving other donors or different superlattice structures.

Unlike *p*-type IID, where the diffusion mechanism was controversial<sup>1,4,5</sup> and was finally clarified as a series of interstitial-substitutional kick outs,<sup>6-8</sup> *n*-type IID is generally thought to be assisted by group-III vacancies. Nevertheless, the microscopic mechanisms of impurity and vacancy motion and the reasons for the enhancement of interdiffusion are still unclear. We thus investigate the energetics of various possible Si diffusion mechanisms and search for the lowest energy pathways. The mechanism by which Si enhances the interdiffusion of Ga and Al atoms involves a Si-vacancy pair and is thus completely different from that of acceptor-induced IID for the same GaAs/AlAs superlattice. It is operative regardless of the method of Si incorporation and therefore explains the difference between the *n*- and *p*-type IID. The computed activation energies are in very good agreement with experimental data.

The simulations were performed using the Car-Parrinello methodology.<sup>9</sup> The electrons are described in the local-density approximation, using norm-conserving pseudopotentials<sup>10</sup> modified to avoid a ghost Ga state.<sup>11</sup> Because of the large activation energies for Si diffusion and group-III atom interdiffusion, a direct *ab initio* molecular-dynamics simulation of these processes is not feasible at present. Instead, we investigate individual mechanisms and determine their activation energies. The formation energies are obtained from total-energy calculations, while migration energies are extracted from total-energy differences between the saddle points and the initial states of the diffusing atom or complex. Most calculations include plane waves with kinetic energies smaller than 14 Ry. For some high-energy mechanisms, an 8-Ry cutoff was used. All calculations were carried out in a 64-atom supercell and all atoms were fully relaxed.

The diffusion of Si through GaAs is the rate-limiting step in interdiffusion, because diffusion in GaAs is slower than  $\text{Al}_x\text{Ga}_{1-x}\text{As}$ .<sup>12,13</sup> Therefore, we focus most of our attention on GaAs, and only investigate the corresponding lowest-energy processes in AlAs.

The calculations were carried out for various diffusion mechanisms for both Si and group-III atoms. For any specific mechanism, there is a specific path for the diffusing atom(s) to follow. However, the position of the saddle point, unless determined by symmetry, is usually unknown. As an alternative to a costly point by point calculation of the total energy along the path, we use an "adiabatic trajectory" technique whenever a migration barrier is needed. The main idea is that the diffusing atom moves with a constant, small speed (e.g., thermal speed at 300 K) along the path defined by the mechanism under consideration, while the remaining atoms continuously relax in response to its motion.<sup>6</sup>

The diffusion mechanisms considered here involve point defects and/or impurity-defect pairs. In equilibrium, their concentrations are determined by their formation energies, which depend linearly on the chemical potentials of the atomic reservoirs for the dopant and host atoms and, in the case of charge defects, on the position of the Fermi level. The chemical potentials of Ga and As ( $\mu_{\text{Ga}}$  and  $\mu_{\text{As}}$ ) were computed self-consistently while constraining their sum and difference to the chemical potential of bulk GaAs and its heat of formation, respective-

ly.<sup>14–16</sup> The Fermi level is determined by the electrical neutrality condition at a given dopant concentration and temperature. The formation energies of native defects in GaAs were computed previously.<sup>6</sup> In a nearly stoichiometric GaAs (up to 0.02% stoichiometry deviation), the chemical potentials of Ga and As vary by less than 0.1 eV. Unless stated otherwise, the quoted formation energies are for a nearly stoichiometric GaAs. For Si, its chemical potential is obtained from a bulk calculation.

To simulate laboratory experiments that involve annealing in As overpressure, we also computed the As and Ga chemical potentials from the equilibrium between GaAs and As<sub>4</sub> vapor. First, we obtain the total-energy and the vibrational frequencies of As<sub>4</sub>.<sup>17</sup> The free energy of As<sub>4</sub> at a given temperature is then computed in an ideal polyatomic gas approximation in a standard fashion. Once the As chemical potential is determined, the Ga chemical potential is given by  $\mu_{\text{Ga}} = \mu_{\text{GaAs}} - \mu_{\text{As}}$ . We find that the As chemical potential at 1 atm partial pressure of As<sub>4</sub> and a temperature of 700°C is about 0.3 eV greater than that determined from the “small stoichiometry deviation” condition discussed above, and thus corresponds to an As-rich environment. This result shows that the gas-solid equilibrium is well defined and that the calculations are reliable. However, a precise computation of the gas-solid equilibrium as a function of temperature exceeds the accuracy of local-density-based methods.

Our calculations show that at a donor concentration of  $6 \times 10^{18} \text{ cm}^{-3}$  and at a temperature of 700°C, there are several defects with low formation energies: Ga<sub>As</sub><sup>2-</sup> (1.4 eV), As<sub>Ga</sub> (1.15 eV), and Ga vacancy  $V_{\text{Ga}}^{3-}$  (1.15 eV). The Ga interstitial occupying the tetrahedral interstitial site with As nearest neighbors (Ga<sub>T<sub>As</sub></sub><sup>+</sup>), which is the highest concentration native defect in *p*-type GaAs, has a formation energy of 2.0 eV. Since the antisite defects are unlikely to be mobile at the diffusion temperature, the main mechanism of diffusion should involve  $V_{\text{Ga}}^{3-}$ . However, because the formation energy of Ga<sub>T<sub>As</sub></sub><sup>+</sup> is still relatively low, diffusion involving interstitial Ga, which is the dominant one in *p*-type material, should also be considered.

Because of its amphoteric nature in GaAs, Si can occupy either a Ga or an As site. It is well known that at low and medium concentrations [up to  $6 \times 10^{18}$  (Refs. 1, 18, and 13)], Si resides preferentially on a group-III site and is thus a shallow donor. At higher concentrations, Si<sub>Ga</sub> will be compensated by the shallow acceptor Si<sub>As</sub> except in the vicinity of *pn* junctions, where net-donor concentrations greater than  $2 \times 10^{19}$  have been observed very recently.<sup>19</sup> Our results show that the formation energy of Si<sub>Ga</sub> is substantially lower than that of Si<sub>As</sub> in intrinsic GaAs grown as As<sub>4</sub> overpressure. Therefore, Si will behave mainly as a donor and the material will become *n* type. The formation energies of Si<sub>Ga</sub> and Si<sub>As</sub> become comparable (within 0.1 eV) at *n*-type doping of  $6 \times 10^{18}$ . Further doping will let Si occupy Ga and As sites equally. This is consistent with experimental observations<sup>20</sup> and previous theoretical results.<sup>21</sup> Since the Si-induced

interdiffusion occurs even at concentrations below  $10^{18}$ , we have focused on the diffusion pathways of Si donors.

Several mechanisms for Si diffusion in GaAs were considered. Whenever explicit values for formation energies of Si defect pairs were needed, we assumed *n*-type material with  $n = 6 \times 10^{18} \text{ cm}^{-3}$ .

The dissociative mechanism<sup>22</sup> assumes that after Si has been incorporated into GaAs on a Ga site, a small fraction of Si becomes interstitial through the reaction  $\text{Si}_{\text{Ga}} \rightarrow \text{Si}_i + V_{\text{Ga}}$ . For a neutral Si<sub>Ga</sub>, the barrier is 5.4 eV, see Fig. 1. For Si<sub>Ga</sub><sup>+</sup>, the barrier increases to 6.1 eV. Both of these results were obtained with an 8-Ry cutoff.

The kick out mechanism<sup>23</sup> involves a kick out by an interstitial Ga of a substitutional Si to an interstitial site:  $\text{Si}_{\text{Ga}} + \text{Ga}_i \rightarrow \text{Si}_i + \text{Ga}_{\text{Ga}}$ . Because both Si<sub>Ga</sub> and Ga<sub>i</sub> are donors, the Si<sub>Ga</sub><sup>+</sup>-Ga<sub>i</sub><sup>+</sup> pair has the lowest formation energy (2.0 eV), although its formation is hindered by Coulomb repulsion. The migration energy is 1.9 eV and the activation energy is 3.9 eV. Figure 1 shows the total energy along the kick out trajectory.

Four vacancy mechanisms have been proposed.<sup>18,4–6</sup> In the Si<sub>Ga</sub>-Si<sub>As</sub> pair mechanism,<sup>18</sup> it is assumed that a single substitutional Si is not mobile and only Si<sub>Ga</sub>-Si<sub>As</sub> pairs can move. In this mechanism, Si<sub>Ga</sub> and Si<sub>As</sub> move in successive jumps along the zigzag chain with the help of Ga and As vacancies. Our calculation shows that the binding energy of the substitutional pair is 0.7 eV and the formation energy of the Si<sub>As</sub>-Si<sub>Ga</sub>-V<sub>As</sub> complex is 2.6 eV. The barrier energy for the Si<sub>As</sub> jump to V<sub>As</sub> is 2.5 eV, implying an activation energy higher than 5.1 eV.

In the Shaw mechanism,<sup>4</sup> a V<sub>As</sub>-Si<sub>Ga</sub> pair forms first. Si<sub>Ga</sub> then moves to the V<sub>As</sub> site, which is followed by second-nearest-neighbor jumps of Ga or As. The formation energies are 2.2 eV for (Si<sub>Ga</sub> + V<sub>As</sub>)<sup>0</sup> and 2.1 eV for (Si<sub>Ga</sub> + V<sub>As</sub>)<sup>2+</sup>. The highest barrier occurs when As jumps to the second-nearest-neighbor vacancy, which requires at least 1.8 eV. The activation energies are thus at least 4.0 and 3.9 eV for the 0 and 2<sup>+</sup> charge states, respectively.

The Van Vechten mechanism<sup>5</sup> starts with a Si<sub>Ga</sub> and a third-nearest-neighbor As vacancy, and proceeds through

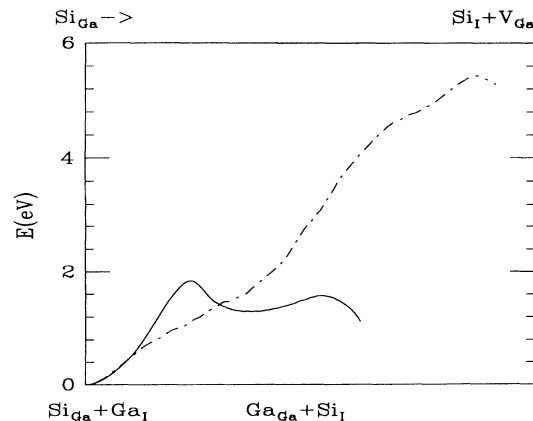


FIG. 1. The total energy for Si motion along the kick out path (solid line, bottom scale) and the dissociative path (dashed line, top scale).

nearest-neighbor jumps. A series of Ga and As jumps must occur before the Si atom can jump. The highest-energy metastable configuration occurs when a string of antisites is generated around a hexagonal ring. Its energy is 5.0 eV above that of the initial state configuration. This shows that diffusion through the Van Vechten mechanism is unlikely.

The  $V_{\text{Ga}}$ -assisted second-nearest-neighbor hopping mechanism<sup>6</sup> starts from a donor-vacancy complex  $(\text{Si}_{\text{Ga}}-V_{\text{Ga}})^{2-}$ . It is a very low formation energy (0.95 eV) in *n*-type GaAs. This agrees well with photoluminescence experiments,<sup>13</sup> which show a very high  $\text{Si}_{\text{Ga}}-V_{\text{Ga}}$  concentration in Si-doped GaAs, and a previous calculation of defect concentrations in Si-doped GaAs.<sup>21</sup> For this mechanism, the saddle point was located by first constraining the Si atom to the plane bisecting the  $\text{Si}_{\text{Ga}}-V_{\text{Ga}}$  path and minimizing the remaining degrees of freedom. Starting from this configuration we performed an adiabatic trajectory simulation in which the Si atom maintained a small constant velocity in the (100) direction while the other degrees of freedom were relaxed using friction forces. The resulting path is shown in Fig. 2(a). Note that it involves Si motion outside the (110) plane. The total energy along this path [Fig. 2(b)] shows a migration barrier of 1.65 eV. A  $V_{\text{Ga}}$  is left behind after the Si hop, and a migration energy of a Ga atom, obtained in the fashion similar to above, is 1.55 eV. This process can be repeated, resulting in  $(\text{Si}_{\text{Ga}}-V_{\text{Ga}})^{2-}$  pair migration through GaAs.  $(\text{Si}_{\text{Ga}}-V_{\text{Ga}})^-$  and  $(\text{Si}_{\text{Ga}}-V_{\text{As}})^0$  complexes

have also been considered, but the  $(\text{Si}_{\text{Ga}}-V_{\text{As}})^{2-}$  complex has the lowest formation and migration energies. The activation energy for Si diffusion through this path is thus  $\sim 2.60$  eV, which is in very good agreement with the experimental values of 2.5–3.0 eV.<sup>25,26,1</sup>

We have also considered the motion of Ga atoms in the absence of Si through the above mechanism. In this case, the migration barrier is 1.9 eV and the saddle point occurs in the plane bisecting the  $\text{Ga}_{\text{Ga}}-V_{\text{Ga}}$  path, slightly outside the (110) plane. In intrinsic, nearly stoichiometric GaAs, the computed formation energy of  $V_{\text{Ga}}^{3-}$  is 2.15 eV, resulting in 4.05-eV activation energy for Ga self-diffusion. The experimental values cluster around 4 and 6 eV,<sup>24</sup> depending in part on sample preparation. However, one should note that fits to the diffusion data using the 4-eV activation energy lead to a very small prefactor, while the operator is true in the case of the 6-eV activation energy. The actual values of the diffusion coefficient are quite comparable in the two cases.

In AlAs, we have only investigated the mechanism having the lowest activation energy in GaAs, namely second-nearest-neighbor hopping of the  $\text{Si}_{\text{Al}}^+-V_{\text{Al}}^{3-}$  pair. Due to the band offset at the GaAs/AlAs interfaces,<sup>29</sup> the Fermi-level effect is more pronounced in the AlAs wells of the superlattice. Taking the theoretical result of 0.6 eV for the band offset and assuming that the chemical potential of As is the same across the interface, the formation energy of the  $\text{Si}_{\text{Al}}^+-V_{\text{Al}}^{3-}$  pair in the AlAs wells is 0.5 eV. Its migration energy is 1.8 eV. Therefore, the activation energy of the second-nearest-neighbor jump mechanism in AlAs is 2.3 eV, which is lower than that in GaAs (2.6 eV). This explains why Si diffusion in GaAs is rate limiting.

The Si-induced disordering thus proceeds with the help of group-III vacancies through the formation of  $\text{Si}_{\text{III}}^+-V_{\text{III}}^{3-}$  pairs, which are bound by Coulomb forces. During the motion of the pair, group-III atoms interchange, leading to the disordering of the superlattice structure. This is in good agreement with the experimental data, such as the photoluminescence signal of the pair following the diffusion,<sup>13</sup> and the fits of the diffusion profiles that led Yu, Tan, and Gösele<sup>26</sup> to conclude that Si-induced interdiffusion is vacancy assisted.

The donor-induced interdiffusion mechanism is thus different from acceptor-induced interdiffusion, where the group-III interstitial kick out contributes the most to dopant diffusion and dopant-induced interdiffusion. The different mechanisms of IID also explain why Si-induced IID occurs both when Si is introduced during the growth of the superlattice and when it is in-diffused from the surface after the growth. For acceptors, such as Zn or Be, IID only occurs during in-diffusion from the surface. In this case, only in-diffusion can generate a nonequilibrium concentration of group-III interstitials through the kick out mechanism, whereas the presence of  $\text{Si}_{\text{Ga}}$  increases the concentration of  $V_{\text{Ga}}^{3-}$  through the so-called ‘‘Fermi-level effect’’<sup>27</sup> and lowers the formation energy of  $\text{Si}_{\text{Ga}}^+-V_{\text{Ga}}^{3-}$  pairs by 0.75 eV through Coulomb attraction. The present results also explain the suppression of Si-induced interdiffusion by Be doping,<sup>28</sup>

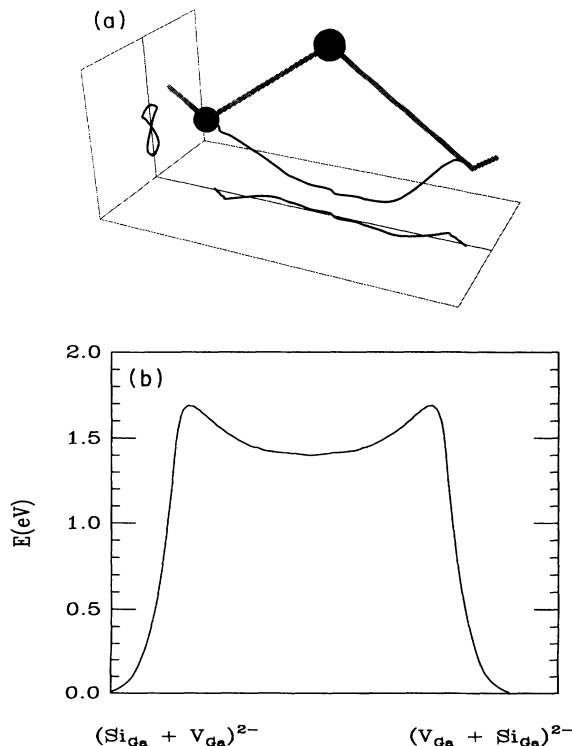


FIG. 2. The second-nearest-neighbor jump of  $\text{Si}_{\text{Ga}}$  to  $V_{\text{Ga}}$ : (a) A three-dimensional view of the Si trajectory; (b) the total energy along the trajectory. See text.

since heavy Be doping lowers the position of the Fermi level and thus increases the formation energies of  $\text{Si}_{\text{Ga}}^+ - V_{\text{Ga}}^{3-}$  pairs.

In summary, we have used *ab initio* molecular dynamics to study Si diffusion in GaAs and the Si-enhanced interdiffusion in GaAs/AlAs superlattices. The results provide a microscopic picture of Si motion in both materials and of the interdiffusion process. The lowest energy diffusion path for substitutional  $\text{Si}_{\text{Ga}}$  involves second-nearest-neighbor jumps assisted by group-III vacancies. Si-vacancy complexes are formed both when Si is introduced during growth and when it is in-diffused from the surface. This is due to the low formation energy of a negatively charged Ga vacancy in *n*-type material and to a Coulomb attraction between the vacancy and an ionized Si donor. The motion of the pair disorders the superlat-

tice regardless of whether Si was introduced during growth or in-diffused afterwards. This is in sharp contrast to acceptor-induced interdiffusion (e.g., by Zn), which requires in-diffusion after growth. The reasons for these differences are due to different diffusion mechanisms and are fully explained by the calculations. We learned very recently that Dr. Dabrowski and Dr. Northrup have independently obtained similar results for the motion of the  $\text{Si}_{\text{Ga}} - V_{\text{Ga}}$  pair.

We want to thank Dr. Boris Yakobson for valuable discussions. This work was supported by ONR, Grant No. N00014-89-J-1827. The calculations were carried out at the Pittsburgh and North Carolina Supercomputing Centers.

- <sup>1</sup>D. G. Deppe and N. Holonyak, Jr., *J. Appl. Phys.* **64**, R93 (1988); T. Y. Tan, U. Gösele, and S. Yu, *Cri. Rev. Solid State Mater. Sci.* **17**, 47 (1991).
- <sup>2</sup>K. Meehan, N. Holonyak, Jr., J. M. Brown, M. A. Nixon, P. Gavrilovic, and R. D. Burnham, *Appl. Phys. Lett.* **45**, 549 (1984).
- <sup>3</sup>M. Kawabe, N. Matsuura, N. Shimizu, H. Hasegawa, and Y. Nannichi, *Jpn. J. Appl. Phys.* **23**, L623 (1984).
- <sup>4</sup>D. Shaw, *Phys. Status Solidi A* **86**, 629 (1984).
- <sup>5</sup>J. A. Van Vechten, *J. Phys. C* **17**, L933 (1984).
- <sup>6</sup>C. Wang, Q.-M. Zhang, and J. Bernholc, *Phys. Rev. Lett.* **69**, 3789 (1992).
- <sup>7</sup>S. Yu, T. Y. Tan, and U. Gösele, *J. Appl. Phys.* **69**, 3547 (1991).
- <sup>8</sup>N. H. Ky, J. D. Ganière, M. Gailhanou, B. Blanxhard, L. Pavesi, G. Burri, D. Araújo, and F. K. Reinhart, *J. Appl. Phys.* **73**, 3769 (1993).
- <sup>9</sup>R. Car and M. Parrinello, *Phys. Rev. Lett.* **55**, 2471 (1985).
- <sup>10</sup>G. B. Bachelet, D. R. Hamann, and M. Schlüter, *Phys. Rev. B* **26**, 4199 (1982).
- <sup>11</sup>X. Gonze, P. Käckell, and M. Scheffler, *Phys. Rev. B* **41**, 12 264 (1990); X. Gonze, R. Stumpf, and M. Scheffler, *ibid.* **44**, 8503 (1991).
- <sup>12</sup>S. Tatsuta, T. Inata, S. Okamura, S. Muto, S. Hiyamizu, and I. Umebu, in *Layered Structures: Epitaxy and Interfaces*, edited by J. M. Gibson and L. R. Dawson, *Materials Research Symposia Proceedings No. 37* (Materials Research Society, Pittsburgh, 1985), p. 23.
- <sup>13</sup>L. Pavesi, N. H. Ky, J. D. Gainère, F. K. Reinhart, N. Baba-Ali, I. Harrison, and B. Tuck, *J. Appl. Phys.* **71**, 2225 (1992).
- <sup>14</sup>S. B. Zhang and J. E. Northrup, *Phys. Rev. Lett.* **67**, 2339 (1991).
- <sup>15</sup>D. B. Laks, C. G. Van De Walle, G. F. Neumark, and S. T. Pantelides, *Phys. Rev. Lett.* **66**, 648 (1991).
- <sup>16</sup>G.-X. Qian, R. M. Martin, and D. J. Chadi, *Phys. Rev. B* **38**, 7649 (1988).
- <sup>17</sup>Our calculated vibrational frequencies for  $\text{As}_4$  are 351, 208, and 265  $\text{cm}^{-1}$  for  $a_1$ ,  $e$ , and  $t_2$  modes, respectively. The corresponding experimental data are 344, 210, and 255  $\text{cm}^{-1}$ , see S. B. Brumbach and G. M. Rosenblatt, *J. Chem. Phys.* **56**, 3110 (1970).
- <sup>18</sup>M. E. Greiner and J. F. Gibbons, *Appl. Phys. Lett.* **44**, 750 (1984).
- <sup>19</sup>A. Vaterlaus, R. M. Feenstra, P. D. Kirchner, J. M. Woodall, and G. D. Pettit, *J. Vac. Sci. Technol. B* **11**, 1502 (1993).
- <sup>20</sup>E. E. Mendez, M. Heiblum, R. Fisher, J. Klem, R. E. Thorne, and H. Morkoç, *J. Appl. Phys.* **54**, 4202 (1983).
- <sup>21</sup>J. E. Northrup and S. B. Zhang, *Phys. Rev. B* **47**, 6791 (1993).
- <sup>22</sup>F. C. Frank and D. Turnbull, *Phys. Rev.* **104**, 617 (1956); R. L. Longini, *Solid State Electron.* **5**, 127 (1962).
- <sup>23</sup>U. Gösele and F. Morehead, *J. Appl. Phys.* **52**, 4617 (1981).
- <sup>24</sup>T. Y. Tan, H. M. You, S. Yu, U. M. Gösele, W. Jäger, D. W. Boeringer, F. Zypman, R. Tsu, and S.-T. Lee, *J. Appl. Phys.* **72**, 5206 (1992).
- <sup>25</sup>P. Mei, H. W. Yoon, T. Venkatesan, S. A. Schwarz, and J. P. Harbison, *Appl. Phys. Lett.* **50**, 1823 (1987).
- <sup>26</sup>S. Yu, U. M. Gösele, and T. Y. Tan, *J. Appl. Phys.* **66**, 2952 (1989).
- <sup>27</sup>T. Y. Tan and U. Gösele, *J. Appl. Phys.* **61**, 1841 (1987).
- <sup>28</sup>M. Kawabe, N. Shimizu, F. Hasegawa, and Y. Nannichi, *Appl. Phys. Lett.* **46**, 849 (1985).
- <sup>29</sup>C. G. Van de Walle and R. M. Martin, *Phys. Rev. B* **35**, 8154 (1987).

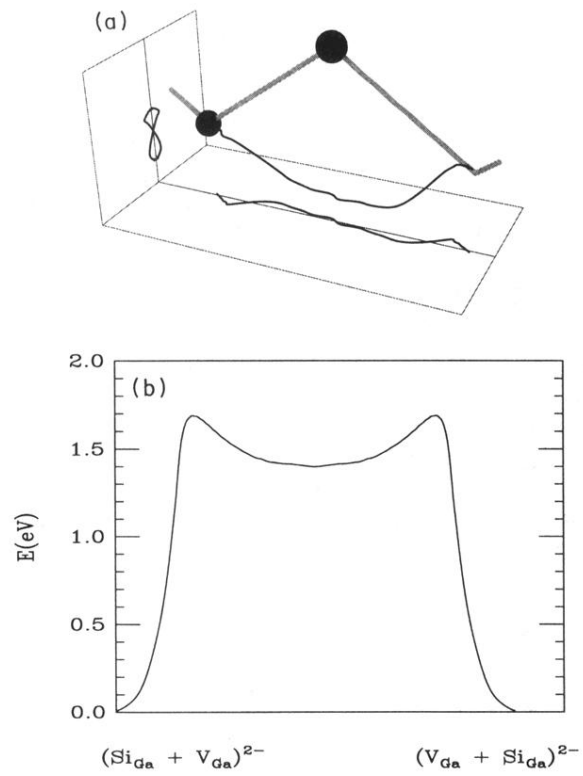


FIG. 2. The second-nearest-neighbor jump of  $\text{Si}_{\text{Ga}}$  to  $\text{V}_{\text{Ga}}$ : (a) A three-dimensional view of the Si trajectory; (b) the total energy along the trajectory. See text.